THE MAGMATIC ACTIVITY ON ASTEROIDS

LESZEK CZECHOWSKI

Institute of Geophysics, University of Warsaw, Poland

Abstract. The tidal effects on a fractured asteroid are considered. The asteroid is assumed to consist of two parts. In gravitational field of another body the motion of one part of the asteroid in relation to second part may be initiated. The necessary conditions for this motion are determined and amount of heat that can be generated is calculated for some cases. It is suggested that metamorphic episodes found in some meteorites are the results of such heating.

1. Introduction

An impressive description of active volcanoes on asteroids was made in 1946 (cf. Saint Exupery, 1946) but most scientists have remained sceptical. There are some reasons for this scepticism. Although the initial temperature of asteroids might be high as a result of energy released during accretion and the decay of short-lived radioactive elements, the rate of heat loss for minor bodies is high in relation to their thermal energy. Likewise, the energy input from decay of long-lived radioactive elements is too low to keep the asteroids hot. Therefore it is generally conceded that their temperatures decrease relatively quickly. Even such large bodies as the Moon and Mercury are considered to have been magmatically inactive for the last 3 billion years.

In 1986 El Goresy *et al.* presented data for unequilibrated enstatite chondrites, which they interpreted as ample evidence for a metamorphic episode on the parent body of these meteorites. A 'geothermometer' based on sphalerite compositions in the Yamato 691 meteorite indicated formation of the assemblage at 620 K and 4×10^7 Pa total pressure. This episode occurred about 1.5 billion year ago. From the value of total pressure one can conclude that the radius of the parent body was at least 200 km (El Goresy *et al.*, 1986b). Other facts enable authors to state that this metamorphic episode was "planetary and endogenic and was not induced by impact" (El Goresy *et al.*, 1986a).

It is impossible to explain such an increase in temperature of the parent body interior as a result of passing close to the Sun. Rather, one has to search of another heat sources. Here I discuss another possibility. It is heating of an asteroid as a result of tidal interaction.

It is widely known that calculations of heat dissipation due to gravity forces enabled Peale *et al.* (1979) to forecast the existence of active volcanoes on Jovian satellite Io. They used formula for the energy dissipation in the form

$$\frac{dE}{dt} = k\frac{f}{Q} ,$$ (1)

where k is the Love's number of the second degree, Q is the tides' dissipation coefficient and f is a function of parameters of satellite orbit. For an almost rigid body (such as an asteroid) $k/Q < 10^{-6}$ and the dissipation of energy calculated from the above formula is negligible (Szeto, 1983).

The situation changes if we assume that asteroid is fractured. Therefore I consider an asteroid (here referred to as satellite) as consisting of two parts. This fractured satellite moves in a gravitational field of another asteroid or planet (here referred to as central body). During this motion the forces with which the central body acts on two parts of the satellite are not equal. If the difference of these forces (per unit of mass) exceeds a critical value the motion along the fault plane begins and heat is generated due to friction force. This effect will be referred to as FRAT (FRactured Asteroid's Tides). As heating is concentrated in a thin layer the resulting temperature increase may be considerable.

The explanation of the results of El Goresy *et al.* (1986a,b) is one of the primary objectives for this research. The others are to investigate three aspects of the FRAT process: necessary conditions for initiating motion along the fault, efficiency of heat generation due to this motion and changes of orbital motion of the satellite. To achieve these scopes the numerical simulation of FRAT was performed.

2. Equations

The orbital motion of the satellite is described by the second law of dynamics

$$(m_1 + m_2)\ddot{\bar{r}}_s = \bar{F}_1 + \bar{F}_2) ,$$ (2)

where m_1 and m_2 are the masses of the satellite's parts, $\bar{r}_s$ is the position vector of mass center of the satellite, $\bar{F}_1$ and $\bar{F}_2$ are gravitational forces acting from central body on the first and second part of the satellite respectively. As $\bar{r}_s$ is calculated in the frame of reference (x, y) situated in center of mass of the whole system the position vector $\bar{r}_c$ of the central body is given by

$$\bar{r}_c = -\bar{r}_s(m_1 + m_2)/M = -\bar{r}_s m/M) ,$$ (3)

where M is the mass of the central body and $m = m_1 + m_2$ is the mass of the satellite.

The motion of the satellite's parts is considered in relation to the frame of reference (x', y') with origin at $\bar{r}_s$ rotating with the satellite. The y' axis is chosen to be perpendicular to the fault plane – Figure 1A. Moreover the angular velocity vector is assumed to be perpendicular to the plane of orbit. The last assumption made the problem essentially 2-dimensional.

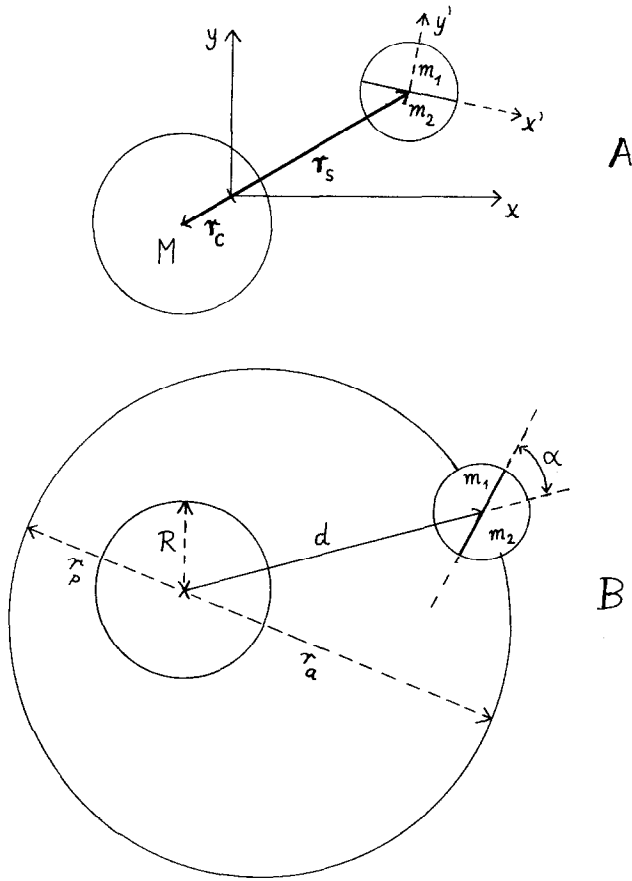The motion of part 1 is given by equation

Fig. 1.   A, Two coordinates frames used in calculation. B, Definitions of the parameters d, R, α.

$$m_1\ddot{\bar{r}}_1 = \bar{F}'_1 + F'_c + \bar{F}'_g + \bar{P} - m_1\ddot{\bar{r}}_s ,\tag{4}$$

where $\bar{r}_1 = (x'_1, y'_1)$ is the radius vector of the centre of mass of part 1 of the satellite in relation to frame (x', y'), $\bar{F}'_c$ denotes centrifugal force and $\bar{F}'_g$ is the gravitational attraction of part 1 by part 2. The component P_x and P_y of $\bar{P}$ denote friction force and reaction force respectively. The Coriolis and other non-inertial forces proportional to $\dot{r}'_1$ or $\ddot{r}'_1$ are negligible and therefore disregarded. The central body is treated as a sphere, whereas the distribution of mass inside the satellite is approximated by some number of mass points. The values of these masses and their position chosen for present calculation are given in Figure 2A. The gravitational field of the satellite and its moment of inertia are to a quite good approximation those for a spherical body (differences are less than 10% for $x'_1 = 0$). The vectors $\bar{F}'_g$ and $\bar{F}'_1$ are calculated as sums of gravitational forces acting on point masses. The centrifugal force F'_c is given by
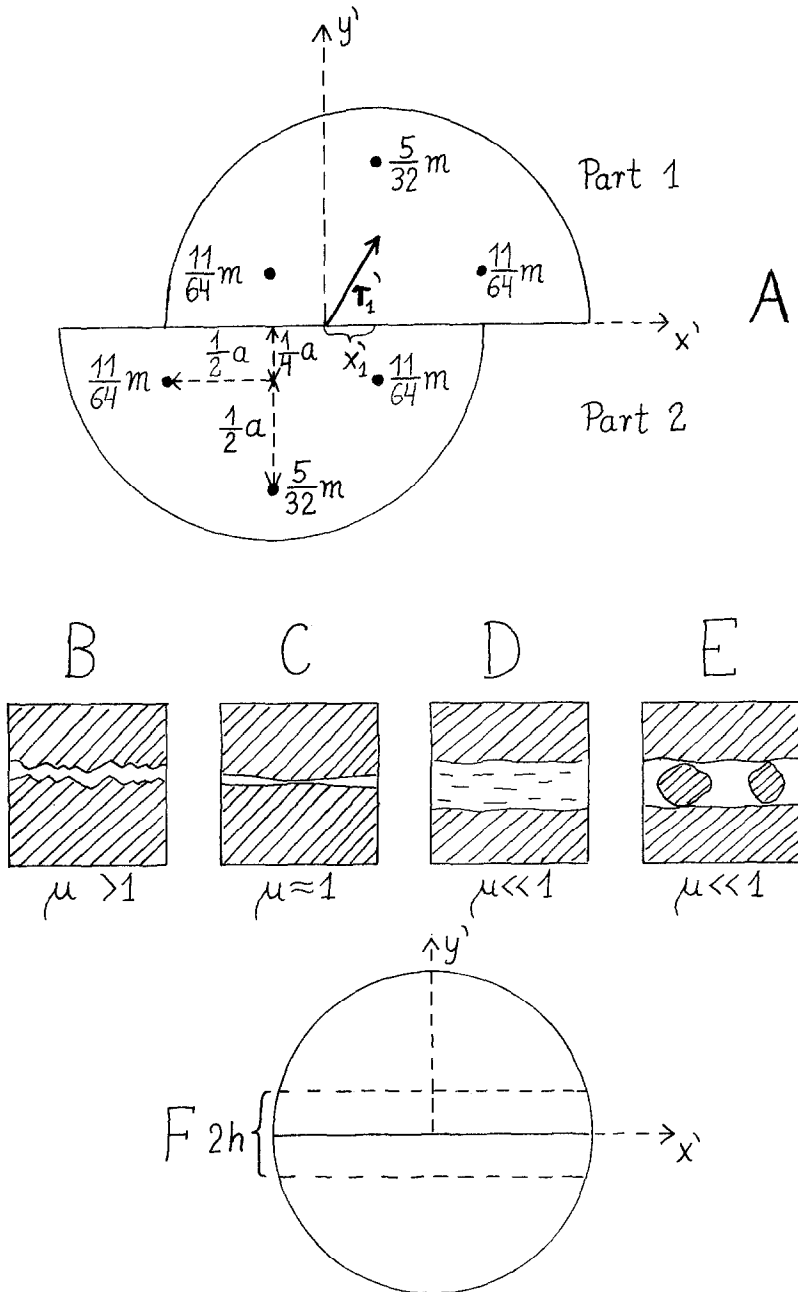
Fig. 2. A, The mass distribution inside the satellite. B, C, D, E, different kinds of faults and corresponding values of the coefficient of friction; F, Thickness of the heated region.

$$\bar{F}'_c = m_1 \omega^2 \bar{r}'_1 \,, \tag{5}$$

where ω is the rotational velocity of the satellite. The energy release is given by

$$\frac{dE}{dt} = |\dot{x}'_1||P_x|\left(1 + \frac{m_1}{m_2}\right) = \mu|\dot{x}'_1||P_y|\left(1 + \frac{m_1}{m_2}\right), \tag{6}$$

where μ is the coefficient of friction and $\dot{x}'_1(1 + m_1/m_2)$ is a velocity of part 1 of satellite relative to part 2.

In the following considerations the dimensionless form of equations is used. This is equivalent to choosing the following units: R (radius of the central body) as a length unit, $(R^3/GM)^{1/2} = (4G\pi\rho/3)^{-1/2}$ as a time unit (t.u.) where $G = 6.67$ 10^{-11} N m^2 kg^{-2} is gravitational constant and ρ is the density of the central body. The mass unit (m.u.) is $M = 4\pi\rho R^3/3$ and GM^2/R is an energy unit (e.u.). As densities of the central body and of satellite are assumed to be equal the radius of the satellite α is given by $\alpha = (A/R) = M^{1/3}$.

3. The Necessary Conditions for FRAT

In this section the necessary conditions for beginning of the FRAT process are considered. The space of parameters of the problem may be divided into 3 regions: region N where motion of part 1 in relation to part 2 cannot begin, region D where satellite is disrupted and region M where motion along fault zone begins without disruption. From Equation (4) we have:

$$\bar{F}'_1 + \bar{F}'_c + \bar{F}'_g + \bar{P} - m_1\ddot{\bar{r}}'_s = 0 \qquad \text{in N region,} \tag{7}$$

$$F'_1 + \bar{F}'_c + \bar{F}'_g + \bar{P} - m_1\ddot{\bar{r}}'_s)\bar{\iota}_y > 0 \qquad \text{in D region,} \tag{8}$$

$$\left.\begin{array}{l}(\bar{F}'_1 + \bar{F}'_c + \bar{F}'_g + \bar{P} - m_1\ddot{\bar{r}}'_s)\bar{\iota}_y > 0 \\ |(\bar{F}'_1 + \bar{F}'_c + \bar{F}'_g + \bar{P} - m_1\ddot{\bar{r}}'_s)\bar{\iota}_x| > 0\end{array}\right\} \quad \text{in M region.} \tag{9}$$

where $\bar{\iota}_x$ and $\bar{\iota}_y$ are versors in frame (x', y'). For given mass distribution inside the satellite's parts (see Figure 2A) we have 6 parameters: distance between satellite and central body – d, angle α between fault plane and radius vector $\bar{r}_c$, coefficient of friction μ, angular spin velocity ω and displacement x'_1.

Let us consider the dependence of the boundaries of the regions on parameters. Figure 3A presents these boundaries for different mass ratios, i.e., $m = 1$, 10^{-3}, 10^{-6}. The main conclusion is that in the coordinates (d, α) the boundaries of the regions are almost insensitive to mass ratio. This somewhat unexpected result may be explained as follows. The gravitational attraction of two parts of the satellite is proportional to a^4 because
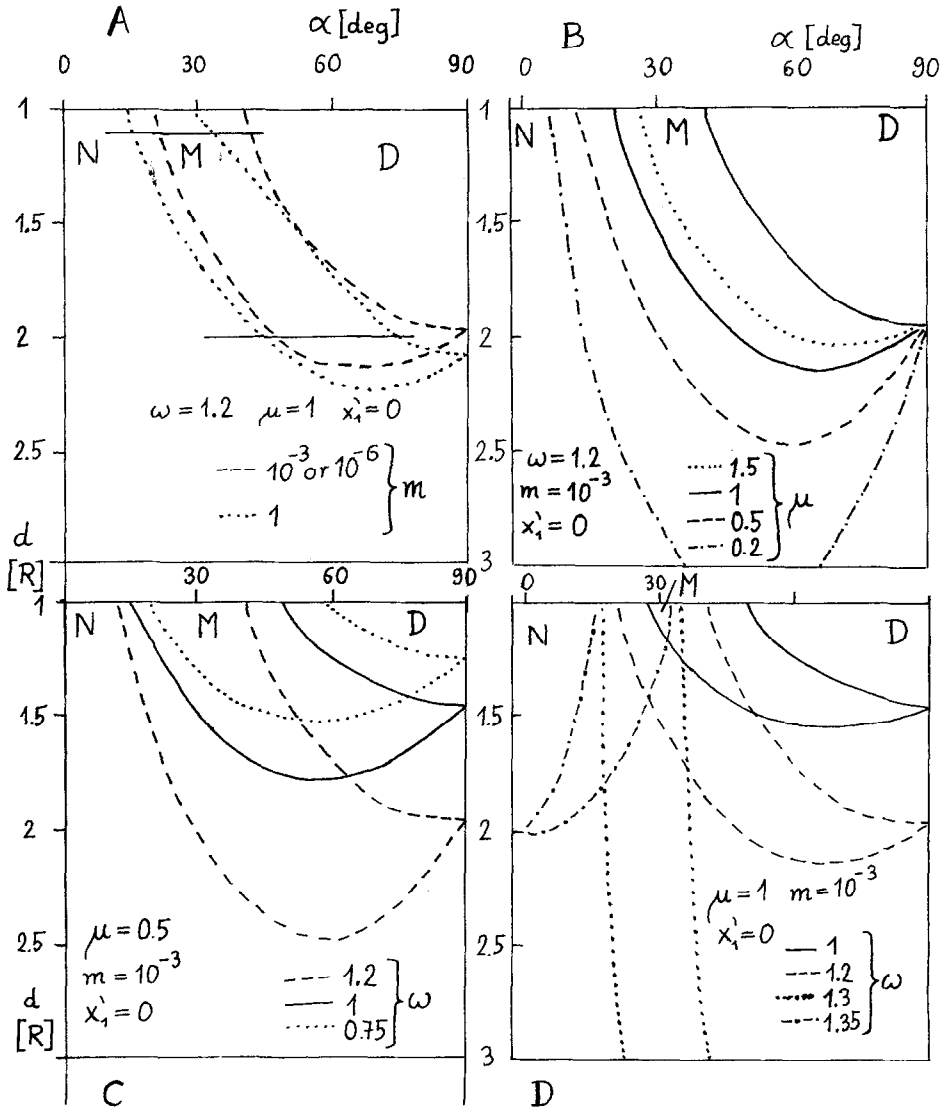
Fig. 3. Regions M, N, D in (d, α) coordinates for different values of the parameters m, μ, ω, x_1'. Regions in Figs. A–D are symmetric in respect to line $\alpha = 90°$, all regions are periodic in α with period 180°.

$$|\bar{F}_g'| \sim \frac{m^2}{\alpha^2} \sim \rho^2 a^4 , \tag{10}$$

The same is true for other forces: centrifugal force F_c': i.e.,

$$|\bar{F}_c'| \sim m\omega^2 |\bar{r}_1'| \sim \rho\omega^2 a^4 ; \tag{11}$$

and 'tidal' force (i.e., $\bar{F}_1 - \bar{F}_2$),

$$|\bar{F}_1 - \bar{F}_2| \sim a \frac{\partial}{\partial d}|\bar{F}_1 - \bar{F}_2| \sim \rho \frac{a^4}{d^3}. \tag{12}$$

The maximum value of friction forces is equal to the y'-component of the sum of these forces multiplied by μ; hence,

$$P_{x\max} \sim a^4. \tag{13}$$

On the other hand the x'-component of the same sum are responsible for the motion along fault plane. Thus the ratio

$$\frac{|P_{x\max}|}{|x\text{-component of the sum}|} \tag{14}$$

is independent of a and consequently of the mass of the satellite as $m = a^3$. This conclusion is not true if $|\bar{r}_s|$ is used instead of d. It should also be noted that for large satellites (i.e., for $a \approx 1$) the Equation (12) is rough approximation and in this case there are some differences in regions' boundaries for $m = 1$ and $m \ll 1$ – see Figure 3A.

The dependence of the boundaries of the friction coefficient μ is presented on Figure 3B. As one may have expected for increasing μ the region M systematically decreases whereas region D is unchanged. More interesting is the fact that even for large μ the region M covers larger range of distance d than region of disruption does. This means that for any μ there are some orbits for which motion along faults can originate but disruption would be impossible for any α if other parameters are unchanged.

Now let us discuss the role of the angular spin velocity ω. It may be seen from Figure 3C that the regions are very sensitive to ω. In fact for $\omega = 0$ the regions D and M almost disappear. On the other hand for large ω the centrifugal force may exceed gravity force $\bar{F}_g$ and consequently disruption occurs even in the absence of tidal forces. This critical value of $\omega_{\max}$ can be obtained from the equation

$$m\omega_{\max}^2|r_1| = |\bar{F}_g \cdot \bar{r}_1||\bar{r}_1|^{-1}. \tag{15}$$

At large distance $\omega_{\max}$ is the largest possible value of spin velocity. For mass distribution used in present calculations $\omega_{\max}$ is equal to 1.3034 rad/t.u. for $x'_1 = 0$ and decreases for increasing x'_1. However close to central body for some range of α the tidal forces help to keep both parts of satellite together and ω may achieve slightly supercritical values – Figure 3D.

The last of discussed parameters is displacement along fault – x'_1. Its role may be significant: e.g., distinct asymmetrical deformation of M and D regions appear for x'_1 as small as 0.005 and dramatically increases for larger x'_1 – Figure 3E. As change of x'_1 is coupled with change of shape of the satellite the similar effects should be observed for satellites of more irregular shape. For most of presented calculations x'_1 is usually less than 0.001 and its effect is not prominent but on the other hand in a few cases x'_1 is comparable to radius of the satellite.
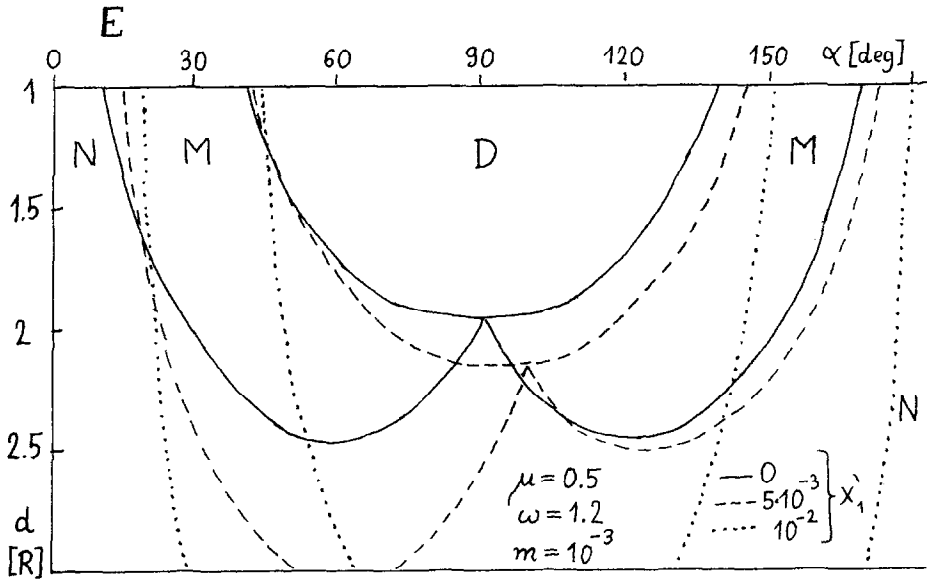
Fig. 3E.

4. FRAT for Close Up

In this section I consider the heat generation during single close up of satellite to central body. As number of unknown parameters is larger than in the previous section the calculations are limited to parabolic orbits and some chosen values of other parameters. The mass of the satellite is taken to be $m = 10^{-3}$. The case $m \approx 1$ and consequently $a \approx 1$ is less interesting because then the accessible part of region M is greatly reduced as minimal possible distance is $1 + a$.

For $m \ll 1$ we can introduce a simple scaling law. Let us note that for $m \ll 1$ $r_s(t)$ is not dependent on m. According to (13) the forces are proportional to a^4. Hence the x'_1 – component of the acceleration of the part 1 of the satellite is given by

$$\ddot{x}'_1 \sim \frac{\text{force}}{m_1} \sim \frac{a^4}{a^3} = a \,. \tag{16}$$

Displacement along the fault plane is

$$\Delta l \sim \ddot{x}'_1 (\Delta t)^2 \,, \tag{17}$$

where Δt is time interval during which the satellite is inside the M region. As $\bar{r}_s(t)$ is mass independent this is also true for Δt. Thus eventually energy in e.u. generated due tidal forces is given by

$$E = (\text{forces}) * (\text{displacement}) \sim a^5 \,. \tag{18}$$

This scaling law have been confirmed by numerical calculations. As energy unit

is proportional to R^5 the E in SI units is proportional to fifth power of the satellite radius, i.e., to $(aR)^5$ and is independent of the mass of the central body.

More problems are with the friction coefficient μ. For rough surfaces effective value of μ may exceed significantly 1 – Figure 2B. But even small displacement along fault plane makes the surface more flat and consequently reduces friction coefficient – Figure 2C. Such displacement may be a result of the same collison that is responsible for the fracture.

Intensive motion along the fault plane may result in melting of the satellite's rocks and rapid drop of μ. On the other hand for 'rubble pill' asteroid boulders between fault surfaces may act as ball-bearing strongly reducing effective coefficient of friction – Figure 2E. The effects of non-constant or low μ will be discussed in another paper. For present calculations I assumed $\mu = 0.5$ or $\mu = 1$.

The calculations are performed for several values of the other parameters. The values of initial angular spin velocity ω_0, minimal distance d_{per} and initial angle α_0 are given by

$$\omega_0 = 0.25 * k[\text{rad/t.u.}] \qquad k = 0.1, \ldots, 5 ;$$

$$d_{per} = 1 + 0.2 * j \, [\text{R}] \qquad j = 1, \ldots, 5 ;$$

$$\alpha_0 = 18 * i \, [\text{deg}] \qquad i = 1, \ldots, 10 .$$

Initial displacement $x'_1 = 0$ for all cases. For given ω_0, α_0, x'_1 the satellite is 'launched' from initial position $\bar{r}_{so} = (20.0)$ into a nearly parabolic orbit with given distance in the pericentrum d_{per}. The results are presented in Table I in the following way. For each pair (ω_0, d_{per}) the upper numbers (in D line) are: number of cases (i.e., number of α_0) for which disruption occurs (first number) and total energy dissipated in 10^{-9} e.u. The lower line (M line) presents the same quantities for cases when motion along fault zone took place without disruption. For example: for $\mu = 0.5$, $\omega_0 = 1$, $d_{per} = 1.4$ it is found that for 4 values of α_0 satellite was disrupted, while the total energy dissipated due to FRAT before the disruption is 77×10^{-9} e.u. For another 4 values of α_0, disruption does not occur and the total energy is 1861×10^{-9} e.u. In two cases FRAT was not observed.

From the results we can conclude that:

1. For large ω_0 the close up usually results in a disruption of the satellite. Before disruption a small amount of heat is generated due to FRAT (about 3×10^{-9} e.u.).
2. The most efficient heating is found for intermediate ω_0 $(0.75 \leq \omega_0 \leq 1)$ and small d_{per} $(d_{per} \leq 1.4)$. For $\mu = 0.5$ the largest value of $E = 9.54 \times 10^{-7}$ e.u. occurs for $\omega_0 = 1$, $d_{per} = 1.4$, $\alpha_0 = 126°$. More details for this close up are presented on Figure 4. For $\mu = 1$ the largest $E = 5.46 \times 10^{-7}$ e.u. corresponds to $\omega_0 = 0.75$, $d_{per} = 1.2$, $\alpha_0 = 36°$. No disruption occurs for these cases.

The energy 2–3 times larger would be dissipated probably for a non zero

TABLE I

A. Parabolic orbits, $\mu = 0.5$, $m = 10^{-3} \cdot \Sigma_n E$ in 10^{-9} e.u.

ω_0	d_{per}	1.2		1.4		1.6		1.8		2.0	
		n	$\Sigma_n E$	n	$\Sigma_n E$	n	$\Sigma_n E$	n	$\Sigma_n E$	n	$\Sigma_n E$
1.25	D	10	63	10	37	10	25	10	33	10	21
	M	0	0	0	0	0	0	0	0	0	0
1	D	8	863	4	77	0	0	0	0	0	0
	M	0	0	4	1861	7	142	1	0.1	0	0
0.75	D	3	462	0	0	0	0	–	–	–	–
	M	5	499	4	161	0	0	–	–	–	–
0.5	D	0	0	0	0	–	–	–	–	–	–
	M	8	875	0	0	–	–	–	–	–	–
0.25	D	0	0	0	0	–	–	–	–	–	
	M	8	364	0	0	–	–	–	–		
0	D	0	0	0	0	–	–	–	–	–	–
	M	9	195	0	0	–	–	–	–	–	–

B. Parabolic orbits, $\mu = 1$, $m = 10^{-3} \cdot \Sigma_n E$ in 10^{-9} e.u.

ω_0	d_{per}	1.2		1.4		1.6		1.8		2.0	
		n	$\Sigma_n E$	n	$\Sigma_n E$	n	$\Sigma_n E$	n	$\Sigma_n E$	n	$\Sigma_n E$
1.25	D	10	34	10	15	10	9	10	13	10	6
	M	0	0	0	0	0	0	0	0	0	0
1	D	6	150	3	16	0	0	0	0	0	0
	M	0	0	3	161	2	1.6	0	0	0	0
0.75	D	1	0.004	0	0	–	–	–	–	–	–
	M	4	750	0	0	–	–	–	–	–	–
0.5	D	0	0	0	0	–	–	–	–	–	–
	M	1	16	0	0	–	–	–	–	–	–
0.25	D	0	0	–	–	–	–	–	–	–	–
	M	0	0	–	–	–	–	–	–	–	–
0	D	0	0	–	–	–	–	–	–	–	–
	M	0	0	–	–	–	–	–	–	–	–

initial value of x_1'. In such a case the motion would last continuously between the point A and point F in Figure 4. But values an order of magnitude larger than 10^{-6} e.u. are hardly to be expected. Consequently, heat input due to FRAT during single close up may be probably assessed at (Equation 18)

$$E \le C(aR)^5 = CA^5 , \tag{19}$$

where $A = aR$ is radius of the satellite in SI units and constant C is equal to 10^{-3} J/m^5.

3. The FRAT effect is very sensitive to d_{per} and μ. For $\mu = 0.5$ FRAT without disruption occurs in 50% of cases if $d_{per} = 1.2$ and only in 1.6% for $d_{per} = 1.8$. The same number for $\mu = 1$ are: 8% for $d_{per} = 1.2$ and less than 1% for $d_{per} = 1.8$.

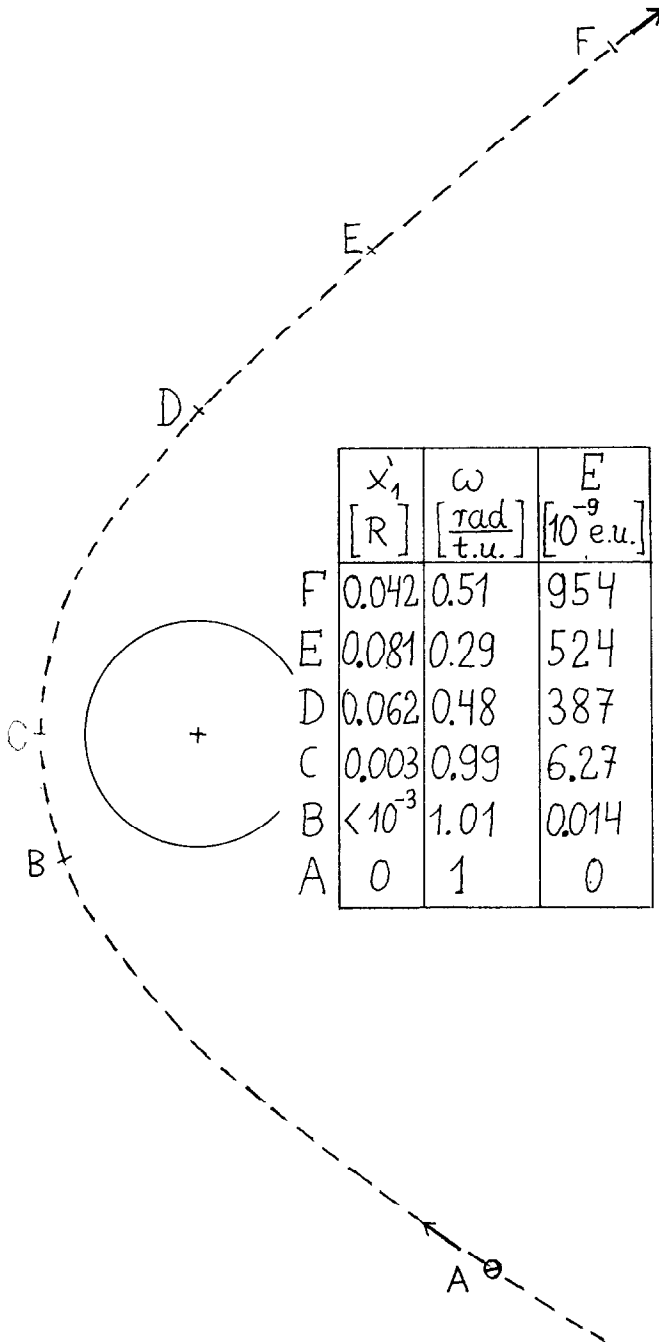|	x'_1 [R]	ω $\left[\frac{rad}{t.u.}\right]$	E $[10^{-9} e.u.]$
F	0.042	0.51	954
E	0.081	0.29	524
D	0.062	0.48	387
C	0.003	0.99	6.27
B	$<10^{-3}$	1.01	0.014
A	0	1	0

Fig. 4. An example of close up for: $\omega_0 = 1$, $\mu = 0.5$, $m = 10^{-3}$, $r_{per} = 1.4$. Heat generation begins at point B, C is the pericentrum, maximum of x'_1 is achieved in E, at F heat generation stops. This is the case of largest dissipation of energy. For most of the other cases of close up the x'_1, E and changes of ω are substantially lower.

5. FRAT for Elliptical Orbits

Because the calculations in this case are more computer's time consuming, the calculations are limited to some values of the parameters. Results are presented in Table II and Figure 5.

Let us note that angular spin velocity ω irregularly oscillates due to slightly aspherical shape of the satellite. For parabolic orbits (with some exceptions as that presented on Figure 4) these changes do not exceed 20%, whereas for elliptic orbits ω changes by a factor of 5–10. If after some time ω sufficiently increases the motion along fault plane begins. Energy of rotation is transformed to heat and consequently ω decreases. This feed-back keeps ω in some range thus reducing the probability of disruption. However the feed-back is not perfect and often fails especially for large μ – Table II and Figure 5B.

The amount of the dissipated energy E is usually one or two orders larger than for most cases of the single close up, as may be expected. On the other hand the largest value of energy for elliptical orbit is only 5 times larger than for single close up. From theoretical point of view the total amount of dissipated energy may be comparable to the difference of initial orbital energy and energy of some final orbit for which FRAT cannot work. However for a given orbit it is difficult to tell whether FRAT is possible because of irregular changes of ω. For some cases there were several periods of peace that lasted for thousands of time units but afterwards motion along fault plane occurred – Figure 5A and B. On the other hand other facts indicate that the orbit really evolves towards the final one. These are: decrease of eccentricity from initial 0.45 to 0.43 and increase of the distance d in pericentrum to 1.525. The further evolution of this 'final' orbit is a result of 'classic' tides.

6. Temperature Increase

The energy released due to friction forces results in the temperature increase. For this consideration it is more convenient to use SI units for all quantities. The thickness of the heated region h could be estimated from the equation of heat conduction. If τ is the duration of heating and κ the coefficient of temperature diffusion then (e.g., Potter, 1973)

$$h = \sqrt{\kappa \tau} \,,$$

thus if we assume that area of the fault is $\pi(aR)^2$ the heated volume becomes (see Figure 2F)

$$V = 2\pi(aR)^2\sqrt{\kappa \tau} = 2\pi A^2 \sqrt{\kappa \tau} \,, \tag{20}$$

where a and A denote the radius of the satellite in $[R]$ and in SI unit respectively. Thus the temperature is increased by
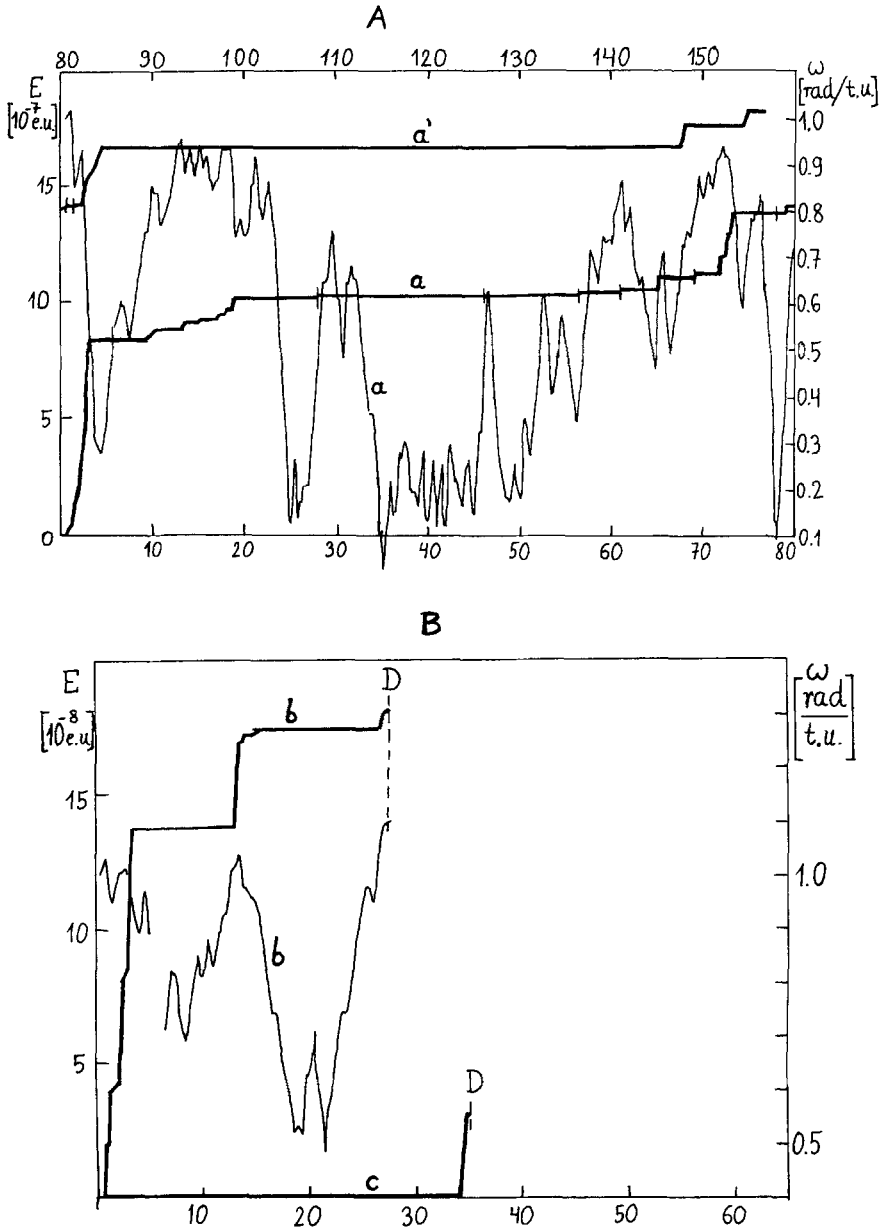
Fig. 5. A, B. Some examples of changes of E and ω (vertical scales) versus number of revolution (horizontal scales). Thick lines are for E, thin one for ω, D denotes moment of disruption. Lines labelled by a, b, c corresponds to cases ($\omega = 1$, $\mu = 0.5$, $d_{per} = 1.5$), ($\omega = 1$, $\mu = 1$, $d_{per} = 1.5$) and ($\omega = 0.5$, $\mu = 1$, $d_{per} = 1.4$) respectively (see Table II). The upper thick line labelled by a' is a continuation of the line α: For it the upper scale should be used. Note: irregular changes of ω, correlations between drops in ω and increases of E and the case c for which heat generation begins only after 33rd revolution.

TABLE II

Results for elliptic orbits, $m = 10^{-3}$, $d_{max} = 4$

μ	ω_0	d_{per}	t in t.u.	E in e.u.	Remarks
1	0	1.2	500	0	
	0.5	1.4	962	$3.07\ 10^{-8}$	disrup.
	1	1.5	763.7	$1.81\ 10^{-7}$	disrup.
	0.5	1.4	500	$1.19\ 10^{-7}$	$d_{max} = 3$
0.5	0	1.2	382	$7.85\ 10^{-7}$	disrup.
		1.4	391	0	
	0.5	1.4	2237	$6.68\ 10^{-7}$	disrup.
		1.8	1000	0	
	1	1.4	13.4	$1.2\ 10^{-8}$	disrup.
		1.5	19081	$4.83\ 10^{-6}$	
		1.6	1000	0	
		1.8	1000	0	
	1.1	1.8	2000	$1.69\ 10^{-7}$	

TABLE III

ΔT for $R = 200$ km, $A = 20$ km

Time t.u.	h m	E e.u.	T K
10^2	0.66	10^{-9}	1
		10^{-8}	10
		10^{-7}	104
		10^{-6}	1040
10^3	2.09	10^{-9}	0.3
		10^{-8}	3.3
		10^{-7}	32.9
		10^{-6}	329
10^4	6.61	10^{-9}	0.1
		10^{-8}	1
		10^{-7}	10
		10^{-6}	104

Time – from beginning of heating, h – thickness of heated region.

$$\Delta T = \frac{E\,(\text{e.u.})}{2\pi\rho c(aR)^2(\kappa\tau)^{1/2}} = \frac{EGM^2}{2\pi\rho c(\kappa\tau)^{1/2}A^2},\tag{21}$$

where E is dimensionless energy from Table I or II and e.u. is the energy unit equal to $GM^2/R = (4\pi\rho/3)^2 GR^5$.

The temperature increase calculated from Equation (21) for $R = 200$ km, $\rho = 3000$ kg/m^3, $\kappa = 10^{-6}$ m^2/s and specific heat $c = 1300$ J/(kg K) is given in Table III. From Equations (18) and (21) we obtain the following scaling law

$$\Delta T \sim (aR)^3 = A^3\,.\tag{22}$$

Thus if $m/M \ll 1$ the temperature increase is proportional to cube of the satellite's radius.
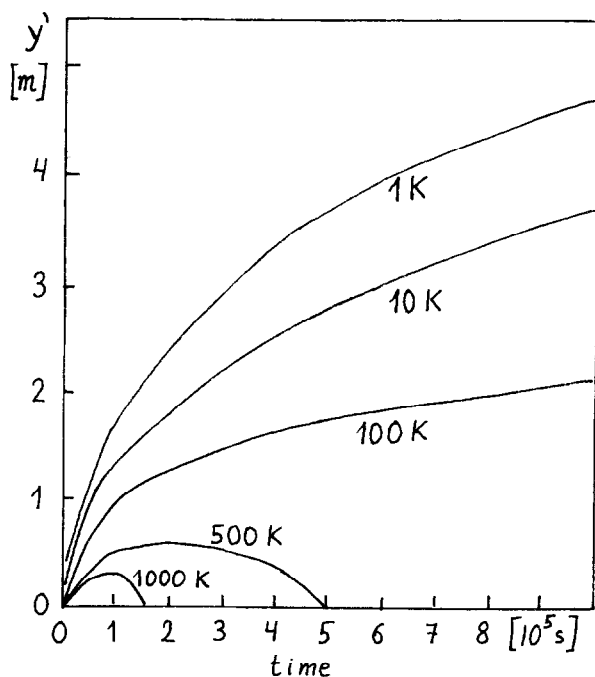
Fig. 6.   Isotherms for the case presented on Figure 4. On vertical scale is the distance of isotherm from the fault plane at given moment of time (horizontal scale).

Equation (21) gives a quite good assessment of mean temperature especially for larger t. However, in order to obtain better insight into the temperature distribution the equation of heat convection was solved for the case of most efficient heating for parabolic orbit – Figure 6.

7. Discussion

The above calculations show that tidal forces may produce considerable amount of heat in fractured asteroids. The question about the probability of such process arises. It requires rather special situation, i.e., fault with moderate effective friction coefficient and large asteroid (or planet) as a central body. We have no direct observational evidence that asteroids are frequently fractured but it is so in the case of Phobos, where the large linear grabens indicate deep faults (e.g., Thomas et al., 1979). Other asteroids are not known with enough details but irregular shape of many others may be a result of frequent collisions. Of course the fracture may be products of these collisions. In fact many investigations have lead to conclusion that disruption and reassembly of asteroids is a common phenomenon and many asteroids are gravitationally bound rubble piles (e.g., Jeffrey et al., 1987; Capaccioni et al., 1986; Davis et al., 1986; Greenberg and Chapman, 1983). The present model of asteroid consisting of two parts may be a good approximation

for reassembled asteroid if one fault plane has significantly smaller friction coefficient than the others. For an 'isotropic' rubble pile other model should be developed.

There is no problem with central body. Orbits of some groups of asteroids cross the orbits of Earth or Mars and consequently their close up are possible. In 1937 the close up of Hermes to Earth was observed. Phobos and Deimos are examples of asteroids moving on elliptical orbits around the planet. It should be also noted that Binzel and Van Flandern (1979) claimed that some asteroids have satellites themselves. However the results of Gehrels *et al.* (1987) eliminate the possibilities of the satellites larger than 30 km in diameter at large distances from central body (i.e., about $30R$). These results do not affect the present calculations because I consider satellites at smaller distance.

The value of angular spin velocity ω is determined for a number of asteroids (e.g., Weidenschilling *et al.*, 1987). The values as large as 2 rad/hour (which corresponds approximately to 0.6 rad/t.u.) are found for several of them. For such ω the presented mechanism is quite possible. Larger ω also cannot be rejected as ω is subject to changes due to collisions and gravitational interaction with other bodies.

Let us now consider the case of Yamato 691. From the scaling law (22) we see that the temperature increase is proportional to $(aR)^3$. The calculations summarized in Table III are performed for the satellite of 20 km radius. As parent body of Yamato 691 had at least a radius of 200 km the temperature increase is 1000 times large than the values in Table III. The temperature increase necessary for metamorphism of Yamato 691 is about 600 K, thus this metamorphism can be readily explained by friction heating due to tidal forces.

In addition to metamorphism an intensive friction heating may cause melting of rocks in the vicinity of the fault plane. After subsequent cooling this results in welding of asteroid's parts. Thus it might be one of the mechanisms that restore the 'rubble pile' as solid body.

Some changes of the satellite's orbit are also the result of FRAT. For elliptical orbits the effect of FRAT is similar to the effect of 'classic' tides although FRAT cannot result in accurate synchronisation. For parabolic orbits the most interesting problem is whether FRAT can be responsible for dissipation of such amount of the kinetic energy of the satellite that enables it to be captured into an elliptical orbit around planet or asteroid. The question of mechanism that would be able to reduce the asteroid's velocity in respect to a planet is crucial for the hypotheses of asteroid origin of the small satellites (e.g., Hartmann, 1987). The most accepted mechanism is gas drag in primordial circumplanetary atmosphere (Hunten, 1979). Pollack *et al.* (1979). For this mechanism the Martian satellites' encounter velocity must be less than 200 m/s but more probable value is 40 m/s (Hunten, 1979). Can FRAT be an alternative to gas drag? From Equation (22) we obtain that velocity reduction Δv due to FRAT is given by

$$\Delta v \leq 0.6 \times 10^{-3} [1/s] \, A. \tag{23}$$

For the case of Phobos which radius is $A = 10^4$ m the velocity reduction is an order lower than for gas drag, but for larger asteroid FRAT effect can give sufficient Δv. Thus one of the possible scenarios is: capturing of large asteroid that subsequently was disrupted into several parts. Two of these parts, i.e., Phobos and Deimos are preserved to present. Beside many drawbacks this scenario has one advantage: contrary to gas drag mechanism it may have occurred at any time after the planets formation. For planets more distant from the Sun the lower Δv is required especially for small bodies and consequently the role of FRAT is more probable for such cases.

Some aspects of FRAT seems to be worth further investigations. These are:

— 3-dimensional effects.
— FRAT in the comet's nuclei. Due to low density and low temperature of melting and vaporising FRAT may be more effective than for silicate asteroids.
— FRAT in isotropic 'pile up'.

8. Conclusions

1. The FRAT mechanism offers quite reasonable explanation of metamorphism of Yamato 691 meteorite or others for which impact origin is rather doubtful.
2. The FRAT can, at least in principle, be a mechanism of capture of an asteroid by other asteroid. The capture by a planet is less probable.
3. As FRAT produces only a limited amount of heat, it should not be used for explanation of more common effects observed in meteorites.

Acknowledgements

References

Binzel R. P. and Van Flandern, T. C.: 1987, 'Minor Planets: the Discovery of Minor Satellites', *Science* **203**, 903–905.
Capaccioni, F., Cerroni, P., Coradini, M., Martino, M. D. I., Farinella, P., Flamini, E., Martelli, G., Paolicchi, P., Smith, P. N., Woodward, A., and Zappala, V.: 1986, 'Asteroidal Catastrophic Collisions Simulated by Hypervelocity Impact Experiments', *Icarus* **66**, 487–514.
Czechowski, L.: 1986, 'Thermal Convection', in R. Teisseyre (ed.), '*Continuum Theories in Solid Earth Physics*', PWN-Elsevier Sci. Publ. Co., Warsaw-Amsterdam, pp. 351–398.
Davis, D. R., Farinella, P., Paolicchi, P., and Zappala, V.: 1986, 'Catastrophic Disruption of Asteroids and Satellites', *J. Italian Astr. Soc.* **57**, 144.
El Goresy, A., Woolum, D. S., and Ehlers, K.: 1986a, 'Planetary Metamorphic Events in Unequilibrated EH Chondrites', *Lunar and Planet. Sci. Conf.* **XVII** NASA, 202–203.

El Goresy, A., Ehler, K., and Woolum, D. S.: 1986b, 'Unequilibrated Enstatite Chondrites: Estimates of Sizes of Parent Bodies Deduced from Mineral Barometers', presented on symposium *Origin and Evolution of Planetary and Satellite Systems*, in Potsdam G.D.R., Oct. 14th–18th.

Gehrels, T., Drummond, J. D., and Levenson, N. A.: 1987, 'The Absence of Satellites of Asteroids', *Icarus* **70**(2), 247–257.

Greenberg, R. and Chapman, C. R.: 1983, 'Asteroids and Meteorites Parent Bodies and Delivered Samples', *Icarus* **55**(3), 455–481.

Hartmann, W. K.: 1987, 'A Satellite-Asteroid Mystery and a Possible Early Flux of Scattered C-class Asteroids', *Icarus* **71**(1), 57–68.

Hunten, D. M.: 1979, 'Capture of Phobos and Deimos', *Icarus* **37**(1), 113–123.

Jeffrey, G. T., Maggiore, P., Scott, E. R. D., Rubin, A. E., and Keil, K.: 1987, 'Original Structures and Fragmentation and Reassembly Histories of Asteroids: Evidence from Meteorites', *Icarus* **69**(1), 1–11.

Olsson-Steel, D.: 1987, 'Planetary Close Encounter', *Icarus* **69**(1), 51–69.

Peale, S. J., Cassen, P., and Reynolds, R. T.: 1979, 'Melting of Io by Tidal Dissipation', *Science* **203**, 892–894.

Pollack, J. B., Burns, J. A., and Tauber, M. E.: 1979, 'Gas Drag in Primordial Circumplanetary Envelopes: A Mechanism for Satellite Capture', *Icarus* **37**(3), 587–611.

Potter, D.: 1973, *Computational Physics*, J. Wiley and Sons, London.

Saint Exupery, A., de: 1946, *Le Petit Prince*, Librairie Gallimard.

Szeto, A. M. K.: 1983, 'Orbital Evolution and Origin of the Martian Satellites', *Icarus* **55**(1), 153–168.

Thomas, P., Veverka, J., Bloom, A., and Uxbury, T.: 1979, 'Grooves on Phobos: Their Distribution Morphology and Possible Origin', *J. Geophys. Res.* **84**(B14), 8457–8477.

Vickery, A. M. and Melosh, H. J.: 1983, 'The Origin of SNC Meteorites: An Alternative to Mars', *Icarus* **56**(2), 299–318.

Weidenshilling, S. J., Chapman, R. C., Davis, D. R., Greenberg, R., Levy, D. H., and Vail, S.: 1987, 'Photometric Geodesy of Main-Belt Asteroids. I. Light Curves of 26 Large, Rapid Rotators', *Icarus* **70**(2), 191–245.